PNAS RESEARCH ARTICLE | IMMUNOLOGY AND INFLAMMATION OPEN ACCESS

Biosensors for inflammation as a strategy to engineer regulatory T cells for cell therapy

Sebastian Bittner[a,b], Brigitte Ruhland[a,b], Veronika Hofmann[a,b], Lisa Schmidleithner[a,b], Kathrin Schambeck[a,b], Asmita Pant[a,b], Philipp Stüve[a,b], Michael Delacher[c], Bernd Echtenacher[a,b], Matthias Edinger[a,d], Petra Hoffmann[a,d], Michael Rehli[a,d], Claudia Gebhard[a], Nicholas Strieder[a], Thomas Hehlgans[a,b,1], and Markus Feuerer[a,b,1,2]

Edited by Shimon Sakaguchi, Osaka Daigaku, Osaka, Japan; received May 16, 2022; accepted August 19, 2022

Engineered regulatory T cell (Treg cell) therapy is a promising strategy to treat patients suffering from inflammatory diseases, autoimmunity, and transplant rejection. However, in many cases, disease-related antigens that can be targeted by Treg cells are not available. In this study, we introduce a class of synthetic biosensors, named artificial immune receptors (AIRs), for murine and human Treg cells. AIRs consist of three domains: (a) extracellular binding domain of a tumor necrosis factor (TNF)-receptor superfamily member, (b) intracellular costimulatory signaling domain of CD28, and (c) T cell receptor signaling domain of CD3-ζ chain. These AIR receptors equip Treg cells with an inflammation-sensing machinery and translate this environmental information into a CD3-ζ chain–dependent TCR-activation program. Different AIRs were generated, recognizing the inflammatory ligands of the TNF-receptor superfamily, including LIGHT, TNFα, and TNF-like ligand 1A (TL1A), leading to activation, differentiation, and proliferation of AIR–Treg cells. In a graft-versus-host disease model, Treg cells expressing lymphotoxin β receptor–AIR, which can be activated by the ligand LIGHT, protect significantly better than control Treg cells. Expression and signaling of the corresponding human AIR in human Treg cells prove that this concept can be translated. Engineering Treg cells that target inflammatory ligands leading to TCR signaling and activation might be used as a Treg cell–based therapy approach for a broad range of inflammation-driven diseases.

regulatory T cell | T cell engineering | inflammation

Significance

In this study, we developed environment-sensing synthetic biosensors for murine and human regulatory T cells (Treg cells) that bind inflammatory molecules of the tumor necrosis factor (TNF) family and, thereby, translate this inflammatory signal into a T cell receptor (TCR)-like activation program. Treg cell activation by these engineered receptors is therefore triggered in an environmental-dependent manner. Our work provides a novel alternative strategy to engineer Treg cells for cellular therapy of inflammatory diseases in which the disease-driving antigens are unknown. As a proof-of-principle in vivo experiment, we could demonstrate that engineered inflammation-sensing Treg cells protect significantly better than Treg cells missing this biosensor against the development of graft-versus-host disease.

Regulatory T cells (Treg cells) are a pivotal T cell population with various functions in the body. Treg cells foster tolerance against self-antigens, allergens, and commensals, thereby limiting self-reactivity of immune cells and excessive inflammation (1). In the last years, it became evident that Treg cells exert additional functions in safeguarding tissue homeostasis and tissue regeneration (2–5). Therefore, Treg cells are a promising candidate to be used as "living drugs" against autoimmune disorders and in transplantation, and first clinical trials have already proven the safety and efficacy of Treg-based cellular therapies (6–8). Concepts applying the chimeric antigen receptor (CAR) technology to Treg cells are being developed to enhance the potency of adoptive Treg cell therapy (9). Preclinical studies have demonstrated the superiority of engineered Treg cells with a CAR-guided antigen specificity over Treg cells with only a natural polyclonal T cell receptor (TCR) repertoire in reducing alloimmune reactions in graft-versus-host disease (GvHD) and graft rejection after transplantation (10–14). CAR–Treg cells were also effectively tested for the treatment of asthma, hemophilia A, experimental autoimmune encephalitis (EAE), and inflammatory bowel disease (IBD) in preclinical models (15–18).

However, in human autoimmune diseases, the implicated autoantigens, which could serve as potential targets for CAR–Treg cells, are often unknown or vary strongly between individual patients. In addition, in many autoimmune and alloreactive diseases, multiple organs and tissues are affected without a uniform antigen that could be targeted by CAR–Treg cells. In contrast to this, the mediators of inflammation show a high redundancy as well as functional importance for the development of various inflammatory diseases, including autoimmunity and alloreactivity. Especially, cytokines of the tumor necrosis factor (TNF) superfamily are involved in many different inflammatory and autoimmune diseases. For example, therapeutic intervention with TNF receptor (TNFR) activation is an important treatment option for several inflammatory diseases (19). These considerations led us to develop a concept for engineered Treg cell therapy by generating artificial immune receptors (AIRs) that target these inflammatory mediators instead of tissue-specific antigens.

We focused on targets of the TNF superfamily and chose receptors of the ligands LIGHT and $LT\alpha_1\beta_2$, TNFα, and TNF-like ligand 1A (TL1A), as these cytokines have

Author contributions: S.B., T.H., and M.F. designed research; S.B., B.R., V.H., L.S., K.S., A.P., P.S., M.D., B.E., and C.G. performed research; S.B., M.E., P.H., M.R., N.S., and M.F. analyzed data; and S.B., T.H., and M.F. wrote the paper.

Competing interest statement: S.B., T.H., and M.F. are inventors on patent application (patent application no. EP22175091.2) based on technology presented in this manuscript.

This article is a PNAS Direct Submission.

See online for related content such as Commentaries.

[1]T.H. and M.F. contributed equally to this work.

[2]To whom correspondence may be addressed. Email: markus.feuerer@ukr.de.

This article contains supporting information online at http://www.pnas.org/lookup/suppl/doi:10.1073/pnas.2208436119/-/DCSupplemental.

Published September 26, 2022.

pleiotropic roles in numerous autoimmune diseases (19) and are expressed as membrane-bound inflammatory ligands. Preclinical disease models and patient data indicate that LIGHT and $LT\alpha_1\beta_2$ signaling through their corresponding receptors lymphotoxin β receptor (LTBR) and herpesvirus entry mediator (HVEM/TNFRSF14) enhance pathology in IBD, autoimmune hepatitis, asthma, rheumatoid arthritis, multiple sclerosis, and GvHD (20). A role for TL1A and its receptor death receptor 3 (DR3) has been described in a variety of inflammatory diseases. Studies with DR3- or TL1A-blocking antibodies or TL1A- and DR3-deficient mice demonstrated a critical involvement for this receptor–ligand system in the induction and maintenance of chronic inflammation in IBD, arthritis, and EAE (21). Moreover, patient data and genome-wide association studies point to a fundamental impact of TL1A-DR3 in human disease (22). The most prominent member of the TNF family, TNFα itself, has been studied extensively since its discovery in 1984. Its proinflammatory function was revealed in multiple diseases, among them ankylosing spondylitis, IBD, rheumatoid arthritis, psoriasis, systemic lupus erythematosus, and juvenile idiopathic arthritis (23).

AIRs as a synthetic tool for cellular therapy allow Treg cells to sense and target these environmental inflammatory signals and translate them into a CD3-ζ chain–dependent TCR program, enabling Treg cells to fulfill their suppressive and tissue-protective functions, independent of a CAR- or TCR-specific antigen.

Results

Generation and Expression of AIRs. We aimed to engineer synthetic receptors for Treg cells that bind ligands of the TNF superfamily and translate their signal into a TCR-activating program. Therefore, complementary DNA (cDNA) sequences encoding the extracellular and transmembrane domains of the corresponding TNFR family member followed by intracellular signaling domains of CD28 and the CD3-ζ chain were cloned into retroviral vectors, which were used for Treg transduction (Fig. 1*A*). We selected three members of the TNFR superfamily: LTBR, DR3, and TNFR2, all based on the expression of their cognate ligands in inflammatory diseases as described in detail above. As intracellular signaling domains to induce a TCR-like Treg cell activation, the CD3-ζ chain and the CD28

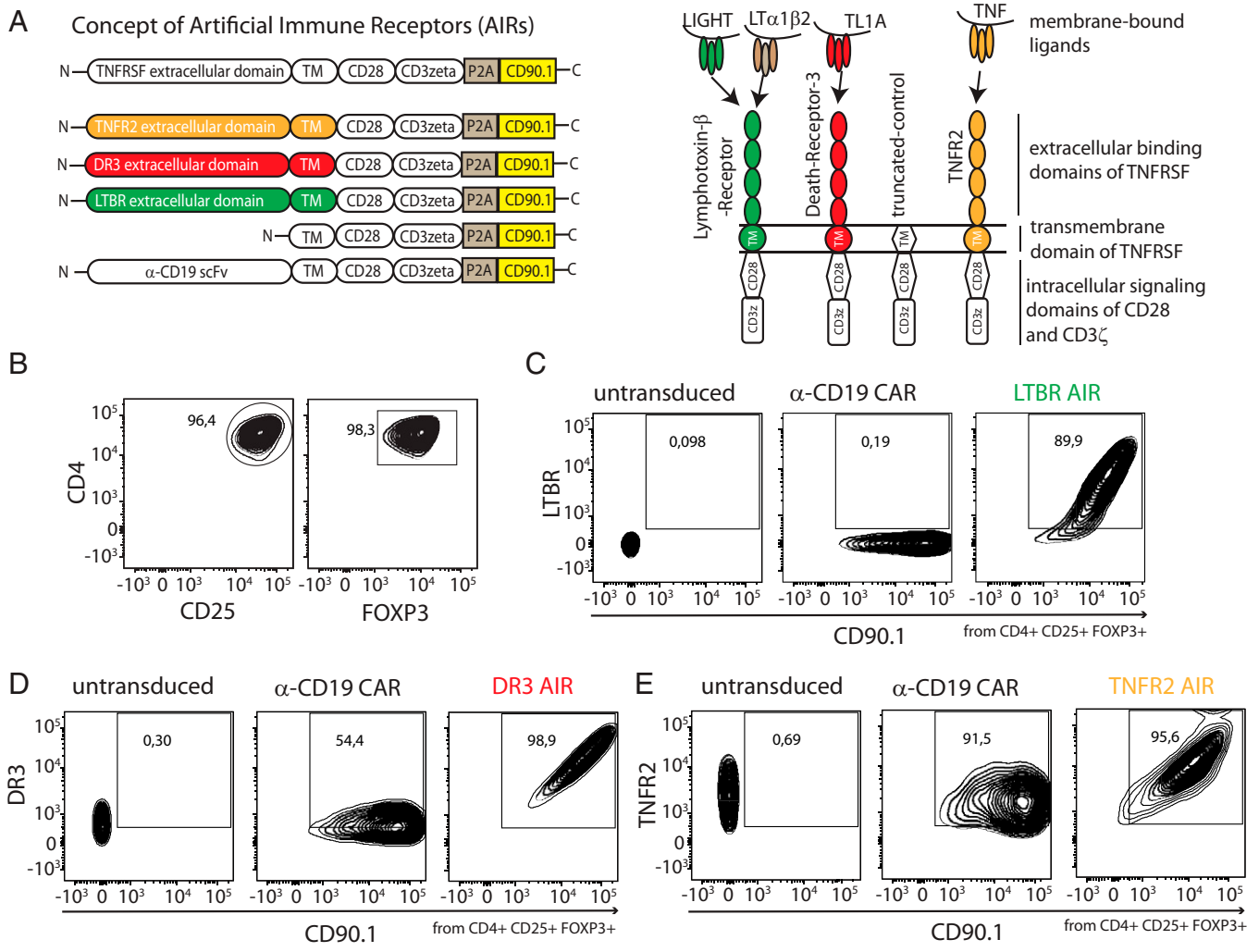

Fig. 1. The concept of artificial immune receptor (AIR) and their expression in primary Treg cells. (*A*) Schematic representation of AIR construct design (*Left*) and of corresponding ligands that induce AIR signaling in a membrane-bound version (*Right*). (*B*) Representative flow cytometric analysis of murine Treg cultures 6 d after sorting. (*C*) Representative flow cytometric analysis of transduction efficiency (CD90.1 expression) and LTBR expression on Treg cells 3 d after transduction with LTBR-AIR, α-CD19 CAR, or on untransduced control Treg cells. (*D*) Representative flow cytometric analysis of transduction efficiency (CD90.1 expression) and DR3 expression on Treg cells 3 d after transduction with DR3-AIR, α-CD19 CAR, or on untransduced control Treg cells. (*E*) Representative flow cytometric analysis of transduction efficiency (CD90.1 expression) and TNFR2 expression on Treg cells 3 d after transduction with TNFR2-AIR, α-CD19 CAR, or on untransduced control Treg cells.

signaling domain were combined as previously reported (10). A self-cleaving P2A peptide linked the AIR protein to truncated CD90.1, which served as reporter for transduction. Murine Treg cells were isolated from spleen and lymph nodes of wild-type C57/BL6 mice or Foxp3-hCD2 reporter mice, sorted to high purity via flow cytometry and transduced during expansion with α-CD3/CD28 stimulation and interleukin-2 (IL-2). Treg cells could be stably expanded under these conditions (Fig. 1*B*). For all three AIR constructs, transduction rates of about 90% were achieved (Fig. 1 *C*–*E*). Treg cells transduced with a retroviral vector expressing an α-CD19 CAR that contained the same intracellular signaling domains as the AIRs were used as a control Treg population. AIR surface expression correlated with CD90.1 marker expression and was detected for LTBR-AIR (Fig. 1*C*), DR3-AIR (Fig. 1*D*), and TNFR2-AIR (Fig. 1*E*). In accordance with literature, expanded and nontransduced Treg cells expressed TNFR2 as well as low amounts of endogenous DR3 (Fig. 1 *D* and *E*), while no LTBR expression was detected (Fig.1*C*), since the LTBR is physiologically expressed by stromal cells, such as fibroblasts, and not by T cells (24).

CD3-ζ Chain–Dependent TCR-like Activation of AIRs. AIRs were designed to bind their respective inflammatory ligands and to translate this into a TCR-like program. To test this, LTBR-AIR Treg cells were coincubated with cells expressing the LTBR-ligand LIGHT. As expression of the transcription factor gene *Nr4a1* is an indicator of immediate-early response of TCR signaling (25), NR4A1 protein expression was measured in LTBR-AIR Treg cells coincubated with endogenously LIGHT-expressing EL-4 cells (26). Intracellular antibody staining revealed NR4A1 upregulation upon LTBR-AIR activation, but not in control Treg cells expressing the irrelevant α-CD19 CAR (Fig. 2*A*). LTBR-AIR–induced NR4A1 expression could be blocked by adding soluble LTBR–immunoglobulin fusion protein, confirming the specificity of the LTBR-AIR-LIGHT interaction (Fig. 2*A*).

To further support these findings, Treg cells from *Nr4a1.eGFP* reporter mice were engineered to express AIRs. AIR signaling capacity was elucidated in coculture experiments with human embryonic kidney (HEK) cells that expressed membrane-bound murine LIGHT (mLIGHT), TL1A, or TNFα (schema in Fig. 2*B*). In order to elaborate the necessity of the CD3-ζ chain for the TCR-like signal in AIR-Treg cells, a mutant version of the LTBR-AIR was generated, lacking the CD3-ζ domain (Fig. 2*C*). AIR-mediated *Nr4a1.eGFP* expression in Treg cells transduced with the CD3-ζ domain mutant and the full-length LTBR-AIR were tested via flow cytometry. *Nr4a1.eGFP* upregulation was found in full-length LTBR-AIR–expressing Treg cells ($CD90.1^+$) after coincubation with HEK-LIGHT cells, but not in Treg cells transduced with LTBR-AIR lacking the CD3-ζ chain (Fig. 2*D*). CD90.1-negative nontransduced Treg cells of the same cocultures or Treg cells transduced with the irrelevant α-CD19 CAR did not upregulate *Nr4a1.eGFP* expression (Fig. 2*D*). Similar to the LTBR-AIR, also TNFR2-AIR and DR3-AIR binding to their corresponding ligands upregulated *Nr4a1.eGFP* expression only in the transduced Treg fraction (*SI Appendix*, Fig. S1 *A* and *B*). TCR activation can induce expression of transforming growth factor (TGF)-β, which remains associated with its propeptide, the latency-associated peptide (LAP), as membrane-bound LAP in Treg cells (10). Therefore, we analyzed whether LAP expression was induced in LTBR-AIR–activated Treg cells. LTBR-AIR coculture with LIGHT-expressing cells induced the expression of LAP (Fig. 2*E*). LAP was not induced in Treg cells transduced with the LTBR-AIR lacking the CD3-ζ chain and the irrelevant α-CD19 CAR Treg cells (Fig. 2*E*). These data indicate that AIR-Treg cells can sense their respective ligands, and this signal is translated into a CD3-ζ chain–dependent TCR-like activation program.

Profound AIR-Mediated Activation of Treg Cells. To analyze AIR-induced changes on gene expression in detail, RNA-sequencing experiments were performed. To this end, LTBR-AIR, DR3-AIR, TNFR2-AIR, or α-CD19 CAR expressing Treg cells from *Nr4a1.eGFP* mice were sorted after coculture with parental or ligand-expressing HEK cells for $CD90.1^+Nr4a1.eGFP^+LAP^+$ or bulk $CD90.1^+$ (Fig. 3*A* and *SI Appendix*, Figs. S2*A* and S3*A*). Unbiased principal-component analysis and differential gene expression analysis revealed profound changes in gene expression in LIGHT-activated LTBR-AIR Treg cells, with 3,709 genes being differentially expressed (Fig. 3 *B* and *C*). LIGHT signaling also induced some changes in gene expression in α-CD19 CAR Treg cells, presumably via the HVEM receptor, which is endogenously expressed on Treg cells (Fig. 3*C*). The LIGHT-induced, LTBR-AIR–specific changes included well-known TCR target genes like *Egr1*, *Egr2*, *Egr3*, *Nr4a1*, *Nr4a2*, *Nr4a3*, and *Irf8* and many genes involved in Treg function, like *Ccr8*, *Ccr6*, *TGFβ1*, *Pdgfβ*, *Tnfrsf9*, *Cx3cr1*, *Lag3*, and *Tigit* (Fig. 3*D* and *SI Appendix*, Fig. S4*A*). Cell sorting and RNA sequencing was also performed for Treg cells activated by DR3-AIR (*SI Appendix*, Fig. S2*A*), revealing specific differential expression of 1,580 transcripts (*SI Appendix*, Fig. S2 *B* and *C*). DR3-AIR signaling included the upregulation of TCR downstream target genes, like of the *Egr* and *Nr4a* family, as well as functional Treg genes that we also detected with the LTBR-AIR construct (*SI Appendix*, Figs. S2*D* and S4*B*). Comparative analysis of TNFR2-AIR to endogenous TNFR-mediated signaling (in α-CD19 CAR Treg cells) on membrane-bound TNFα stimulation revealed a predominant signaling of endogenous TNFR in murine Treg cells (*SI Appendix*, Fig. S3 *A*–*C*), most likely due to high endogenous TNFR2 surface expression. Although a clear discrimination between the RNA profiles was detectable (*SI Appendix*, Fig. S3*B*) and TCR downstream targets like *Nr4a1*, *Nr4a3*, *Irf8*, and *Egr3* were found specifically in the TNFR2-AIR–activated Treg cells (*SI Appendix*, Figs. S3 *C* and *D* and S4 *C*), the artificial TNFR2-AIR signaling and the endogenously expressed TNFR appeared to compete for TNFα, leading to decreased TNFR2-AIR output compared with signals triggered by DR3-AIR and LTBR-AIR in Treg cells. High surface expression of TNFα was detected on the cell membrane of transfected HEK cells, ruling out enzyme-mediated cleavage of membrane-bound TNFα as a possible reason for decreased TNFR2-AIR output (*SI Appendix*, Fig. S3*E*).

As suggested by the dependency of the AIR signaling on the CD3-ζ-domain and the induction of *Nr4a1* expression, the RNA-sequencing (RNA-seq) data confirmed the AIR-induced TCR-like activation program, as many TCR downstream targets were also found in α-CD3/CD28–mediated Treg activation, such as the *Egr* and *Nr4a* family members (*SI Appendix*, Fig. S2 *E* and *F*). From the 2,102 LTBR-AIR upregulated genes, 1,199 (57%) were also found in α-CD3/CD28–stimulated Treg cells (*SI Appendix*, Fig. S2*G*).

AIR Activation Supports Treg Program and Mediates Proliferation. Activation of Treg cells via AIRs led to considerable changes in gene expression, including induction of activation marker, such as *Tnfrsf9* (*Cd137*) and *Cd69*, as well as Treg functional genes, like *TGFβ1*, *Fgf2*, *Penk*, *Tigit*, and *Irf8*, and chemokine receptor genes, such as *Ccr8*, *Ccr2*, and *Ccr6* (Fig. 4*A* and *SI Appendix*, Fig. S4 *A*–*C* and Fig. S5 *A* and *C*). Flow

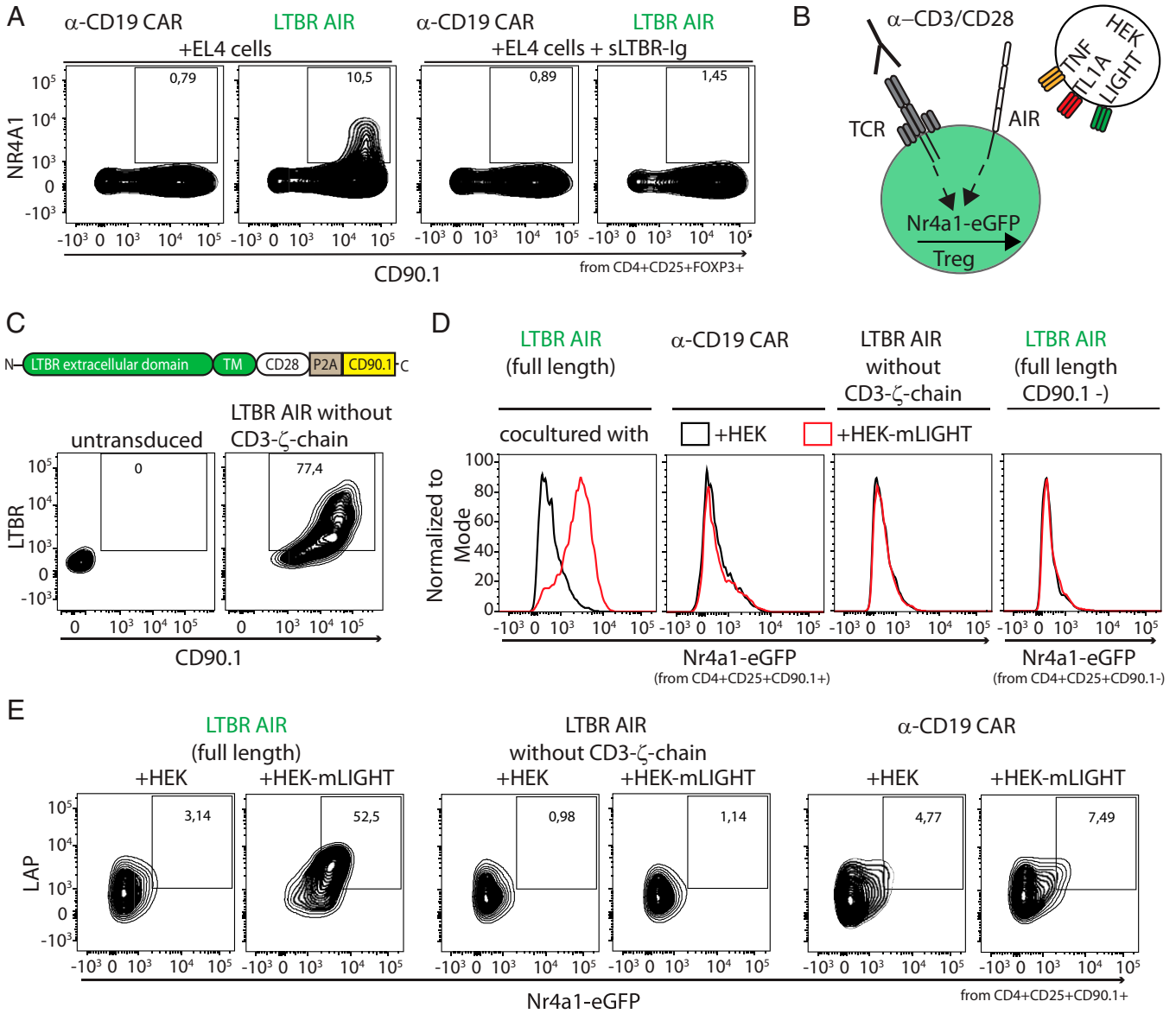

Fig. 2. AIRs induce Nr4a1 upregulation. (*A*) Flow cytometric analysis of LTBR-AIR or irrelevant CAR-expressing Treg cells that were cocultured with irradiated murine EL4 cells for 18 h, in absence or presence of a mLIGHT-blocking LTBR–immunoglobulin fusion protein (50 μg/mL) and afterward stained for intracellular NR4A1 expression. One out of three independent experiments is shown. (*B*) Schematic experimental design: AIR-expressing Treg cells from Nr4a1-eGFP reporter mice were cocultured with HEK cells or HEK cells transiently expressing membrane-bound mTNFα, mLIGHT, or mTL1A in order to analyze AIR capacity to induce NR4A1 expression. (*C*) A version of LTBR-AIR lacking the CD3-ζ chain domain was designed, and surface expression was confirmed via flow cytometry in transduced murine Treg cells. (*D* and *E*) LTBR-AIR, LTBR-AIR without CD3-ζ chain, or α-CD19 CAR–expressing Treg cells from Nr4a1.eGFP reporter mice were rested for 24 h and then cocultured with HEK cells or HEK cells expressing mLIGHT for 18 h and afterward analyzed for eGFP and LAP expression via flow cytometry. One out of two independent experiments is shown.

cytometry analysis of Treg cells, activated via LTBR-AIR (Fig. 4 *B* and *C*) or DR3-AIR (*SI Appendix*, Fig. S5 *B* and *C*), confirmed protein expression of several of these molecules, including CD137, LAP, CD69, TIGIT, and IRF8. Importantly, LTBR-AIR was only stimulated by membrane-bound and not by soluble LIGHT (Fig. 4*D* and *SI Appendix*, Fig. S6*A*). Similarly, also TNFR2-AIR only induced CD137, TIGIT, and Nr4a1 upregulation after binding to its membrane-bound ligand (*SI Appendix*, Fig. S6 *B* and *C*). This quality is prerequisite for Treg activation at the site of inflammation and indicates a local and not systemic mode of action.

The AIR-triggered program illustrated by protein expression of CD137, TIGIT, LAP, and CD69 in Treg cells might resemble a CAR-induced program, as Treg cells transduced with an α-HLA-A2 CAR (containing the same intracellular signaling domains as AIRs) exhibited comparable expression of aforementioned proteins after coculture with HLA-A2-positive PANC-1 cells (*SI Appendix*, Fig. S6*E*).

As TCR or CD3-ζ chain–dependent signaling can initiate T cell proliferation, we tested for the proliferation-inducing capacity of the AIRs. To this end, AIR-Treg cells were generated, labeled with carboxyfluorescein succinimidyl ester (CFSE) and rested without TCR stimulation for 24 h. Labeled, rested AIR-Treg cells were incubated with the respective ligand expressing HEK cells for 72 h, and CFSE dilution was analyzed via flow cytometry. All three AIR constructs led to cell division in response to the corresponding ligand (Fig. 4*E* and *SI Appendix*, Fig. S6 *F* and *G*).

In contrast to the full-length LTBR AIR, the LTBR-AIR lacking the CD3-ζ chain was unable to induce the abovementioned proteins CD69, TIGIT, LAP, and CD137 (Fig. 4*F* and *SI Appendix*, Fig. S6*D*), reconfirming the CD3-ζ chain dependency of the AIR signaling.

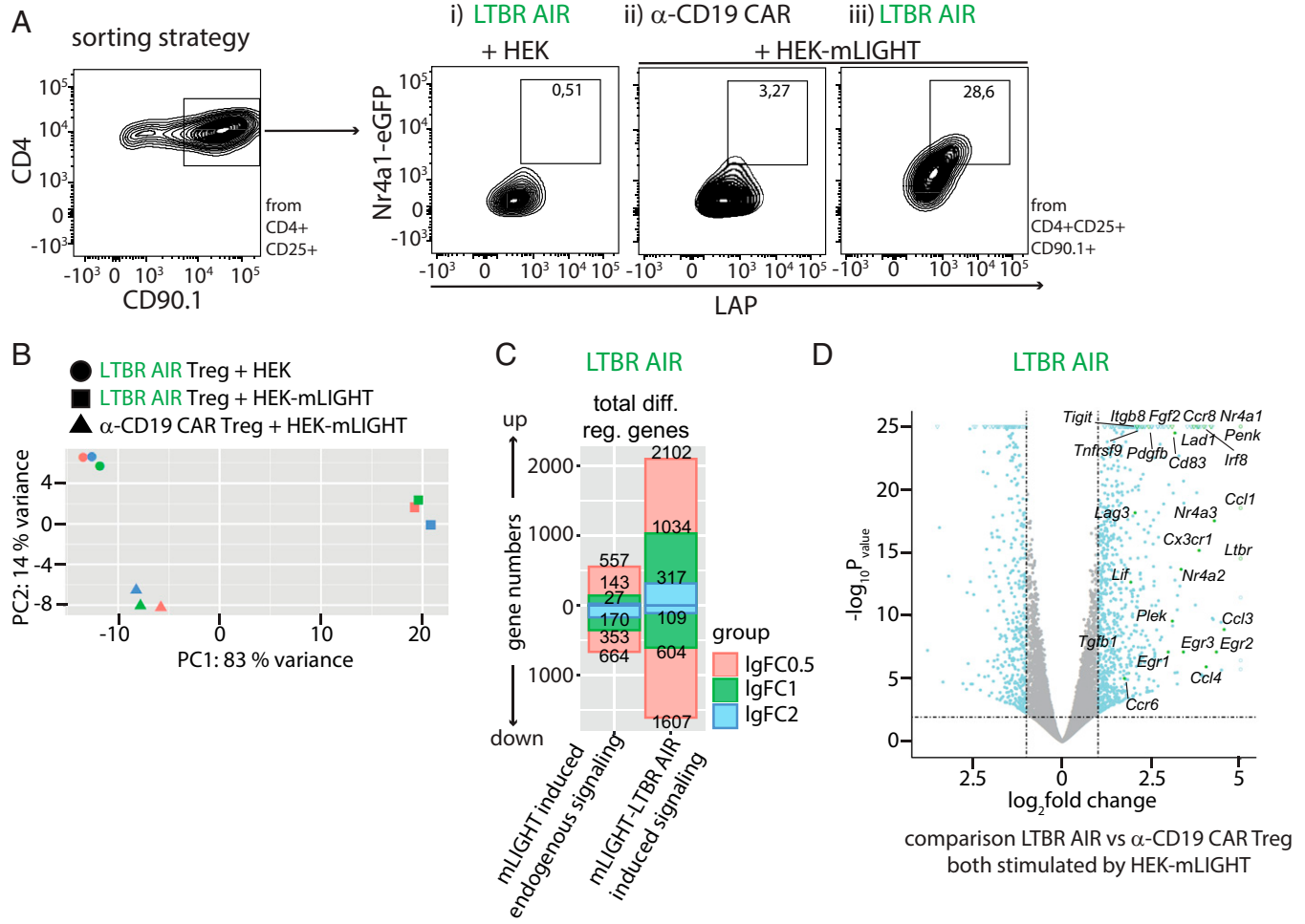

Fig. 3. AIR activation triggers TCR-like signaling. (*A*) LTBR-AIR or irrelevant CAR-expressing Treg cells were rested for 24 h and then cocultured for 18 h with HEK cells or HEK cells expressing mLIGHT. Treg cells were sorted on living $CD4^+CD25^+CD90.1^+$ (conditions: i and ii) or $CD4^+CD25^+CD90.1^+Nr4a1^+LAP^+$ (condition: iii). One representative sorting layout is shown ($n = 3$). (*B*) Principal-component analysis of RNA-seq data of samples generated in *A*. (*C*) Summary of up- and downregulated genes comparing α-CD19 CAR Treg cells stimulated with HEK-mLIGHT versus LTBR-AIR Treg cells stimulated with HEK cells as control (endogenous mLIGHT signaling) and LTBR-AIR Treg cells stimulated with HEK-mLIGHT versus α-CD19 CAR Treg cells stimulated with HEK-mLIGHT (specific LTBR-AIR signaling); lgFC: log fold change. (*D*) Volcano plot showing differentially expressed transcripts after LTBR-AIR stimulation (comparison LTBR-AIR Treg stimulated with HEK-mLIGHT versus α-CD19 CAR Treg stimulated with HEK-mLIGHT).

In summary, AIRs can activate Treg cells in a TCR-like manner in response to binding to their cognate membrane-bound ligands, leading to cell proliferation and induction of molecules relevant for Treg cell function. Those molecules included, for example, the transcription factor IRF8, which is important for the suppressive Treg function (27, 28), or *TGFβ1*, which can support tissue regeneration as well as suppressive Treg function (29).

LTBR-AIR Improves Adoptive Treg Cell Therapy in a GvHD Model. GvHD is a frequent complication after allogeneic bone marrow or hematopoietic stem cell transplantation induced by cotransferred alloreactive donor T cells. Several preclinical studies illustrate a promising perspective for GvHD therapy through the administration of Treg cell products (30, 31). LIGHT inhibition significantly ameliorated GvHD in preclinical models (32, 33), and additionally, upregulation of LIGHT was described in patients suffering from acute GvHD (34). Therefore, as a proof of principle, the potency of AIR-Treg cells for the treatment of an inflammatory disease was tested with the LTBR-AIR construct in a complete major histocompatibility complex (MHC) mismatch model of GvHD as depicted in Fig. 5*A*. To this end, Treg cells (C57BL/6, Foxp3-hCD2 reporter, and congenic CD45.2) expressing the LTBR-AIR or a truncated form of the LTBR-AIR as control, in which the extracellular domain had been deleted, were transplanted into lethally irradiated BALB/c mice together with bone marrow (BM) cells and splenocytes, which included a pool of alloreactive T cells. Quality control of the transduced Treg cells revealed high Treg cell purity (over 95% hCD2/FOXP3 positive) and a transduction rate of over 95% before adoptive transfer (Fig. 5*B*). Blood samples were taken on day 20 after transplantation to analyze B cell frequencies, because failure to reconstitute the B cell compartment is a sensitive indicator for GvHD and Treg-mediated protection from GvHD is reflected in higher B cell counts (31, 35). The B cell compartment was strongly reduced in animals receiving BM and splenocytes (GvHD group) in comparison to animals receiving BM cells only. Control Treg cell–receiving animals showed a tendency for B cell recovery, but only the LTBR-AIR Treg group reconstituted significantly B cells as compared with the GvHD group (Fig. 5*C* and *SI Appendix*, Fig. S7*A*). The survival of mice was monitored, and a clinical GvHD score considering body weight, activity, fur appearance, and other parameters was assessed. Treatment of mice with LTBR-AIR Treg cells resulted in a significantly prolonged survival (Fig. 5*D*) and lower GvHD score, including less-pronounced weight loss,

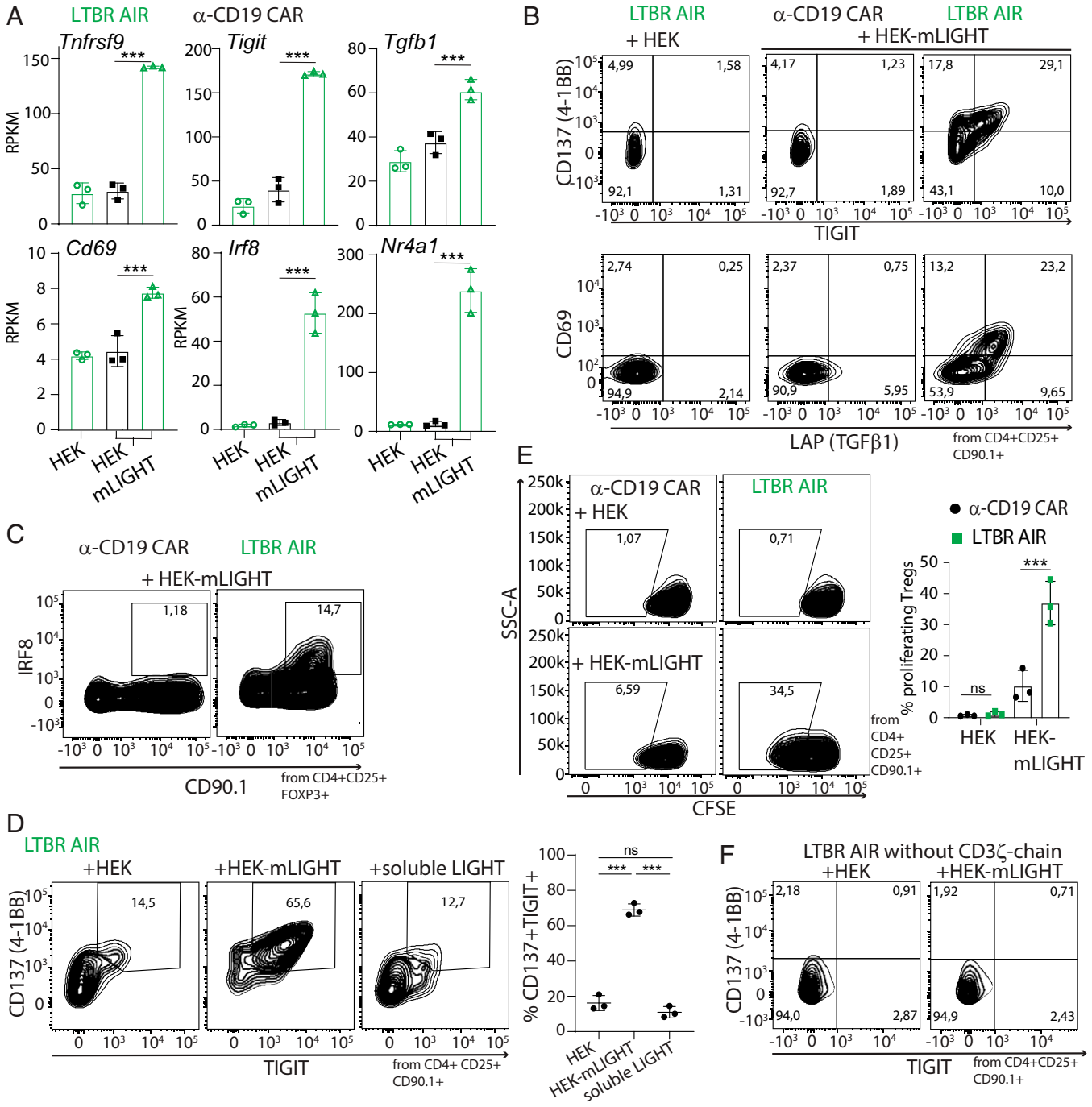

Fig. 4. AIRs mediate Treg activation and proliferation. (*A*) RNA expression data from LTBR-AIR or irrelevant CAR-expressing Treg cells for *Tnfrsf9*, *Tigit*, *Tgfb1*, *Cd69*, *Irf8*, and *Nr4a1* after 18 h coculture with HEK ± mLIGHT (Deseq2, $n = 3$). (*B* and *C*) Flow cytometric analysis from LTBR-AIR or irrelevant CAR-expressing Treg cells after 18 h coculture with HEK ± mLIGHT. Protein expression of CD137 and TIGIT is shown in the *Upper* and CD69 and LAP in the *Lower* panels in *B*. Intracellular IRF8 expression is shown in *C*. Data are representative for four independent experiments. (*D*) Representative flow cytometric analysis from LTBR-AIR Treg cells after 18 h coculture with HEK ± mLIGHT or stimulation with soluble LIGHT (50 ng/mL) on the *Left*. *Right*: summary of three experiments (ordinary one-way ANOVA) ns, not significant; $P > 0.05$. (*E*) LTBR-AIR or control CAR-expressing Treg cells were rested for 24 h and labeled with CFSE proliferation dye. Engineered and labeled Treg cells were cocultured with HEK ± mLIGHT for 72 h in presence of IL-2 and afterward analyzed via flow cytometry for proliferation. Representative dot plots are shown on *Left*. Summarized data from three experiments (mean ± SD) performed in three technical replicates are shown on *Right* ($n = 3$, two-way ANOVA). (*F*) Flow cytometric analysis of CD3-ζ chain lacking LTBR-AIR-expressing Tregs that were cocultured with HEK cells or mLIGHT-expressing HEK cells for 18 h. *$P < 0,05$; **$P < 0,01$; ***$P < 0,001$.

compared with mice receiving no Treg cell therapy or control Treg cells (Fig. 5 *E* and *F*).

Interestingly, transferred AIR-Treg cells (CD45.2$^+$) retained stable FOXP3 expression (*SI Appendix*, Fig. S7*B*, *Left*) and additionally upregulated the expression of KLRG1 (*SI Appendix*, Fig. S7*B*, *Right*), a marker of tissue Treg cell differentiation (5, 36). Both FOXP3 as well as KLRG1 protein expression in engineered AIR-Treg cells was detectable on a similar level as compared with Treg cells originating from the transplanted BM (CD45.1$^+$), indicating differentiation into a tissue-Treg–specific phenotype. This differentiation ability could be relevant, because, among the LTBR-AIR Treg treatment group, those mice that survived until the end of the experiment showed significantly higher frequencies of KLRG1$^+$ LTBR-AIR Treg cells

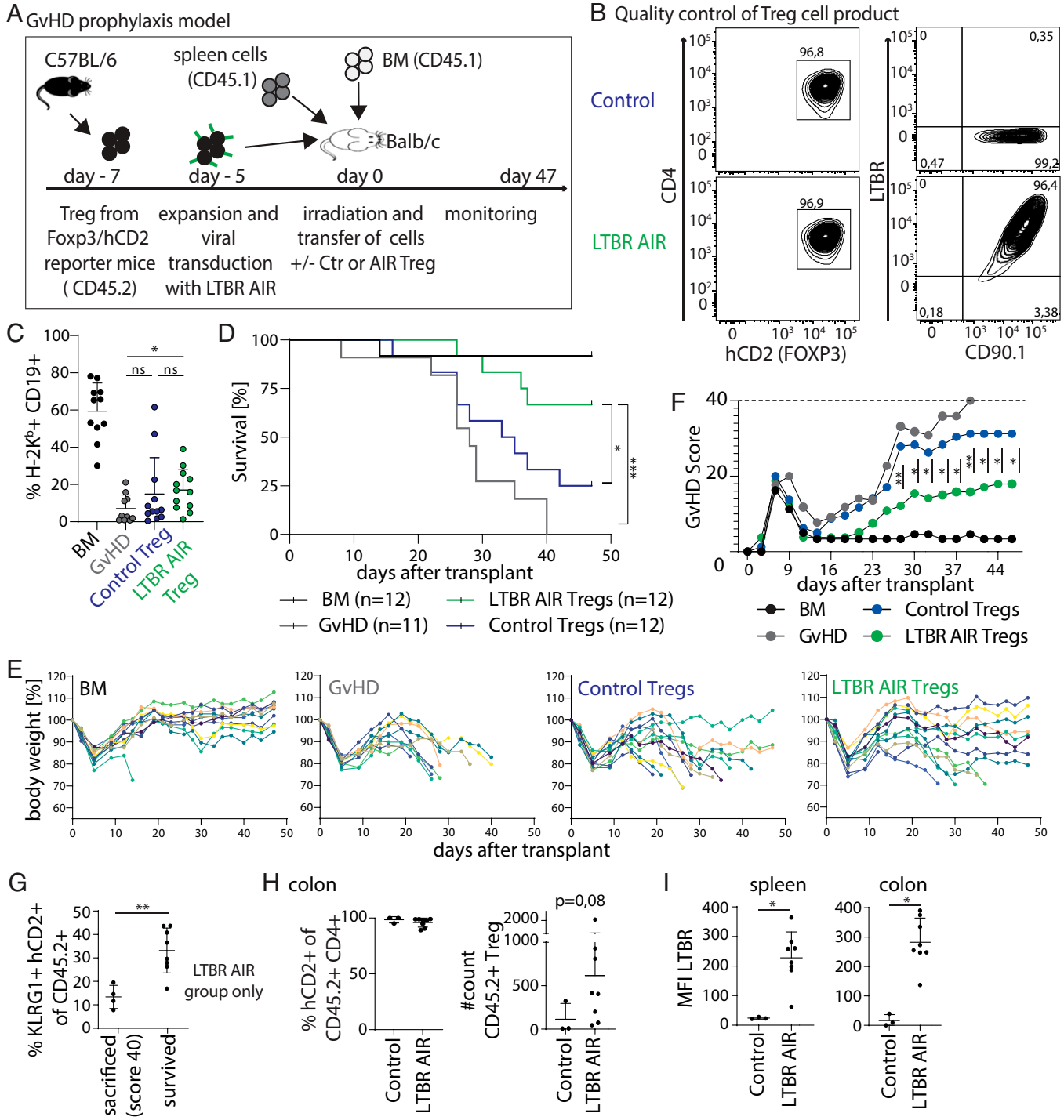

Fig. 5. LTBR-AIR Treg ameliorates GvHD pathology in mice. (*A*) Schematic overview of performed (complete MHC mismatch, C57/BL6 into BALB/c) graft-versus-host disease (GvHD) model. (*B*) Flow cytometric analysis of engineered Treg cells before transfer into mice. (*C*) On day 20, a blood sample from each animal was taken to check for donor-derived (H-2K^b+) CD19$^+$ B cells via flow cytometry (Kruskal–Wallis test, n = 10–12). (*D*) Kaplan–Meier curve showing survival of transplanted BALB/c mice. Graph contains datasets from two independent experiments (log-rank test, n = 11–12). (*E*) Body weight shown for each individual animal. (*F*) Mean GvHD score per group (two-way ANOVA). (*G*) Frequency of KLRG1$^+$ hCD2$^+$ Treg cells in spleens of mice receiving LTBR-AIR Treg cells (Mann–Whitney U test, survivors n = 8, end of experiment day 47) versus sacrificed due to score (n = 4). (*H*) *Left*: percentage of hCD2$^+$/FOXP3$^+$ cells among transferred engineered CD45.2$^+$ cells, isolated from colon, at day 47; *Right*: cell count of transferred CD45.2$^+$ Treg in colon at day 47. (*I*) Mean fluorescence intensity (MFI) for LTBR/PE/Cy7 of CD45.2$^+$CD90.1$^+$ Treg cells isolated from spleen (*Left*) or colon (*Right*, Mann–Whitney U test). *P < 0,05; **P < 0,01; ***P < 0,001.

compared with mice that had to be sacrificed because of GvHD severity (Fig. 5*G*). The intestine is a strongly affected organ in GvHD. LTBR-AIR Treg cells migrated to the colon, were detectable in the colon even 47 d after transfer (end of experiment), and showed stable hCD2/FOXP3 expression (over 90%), as well as KLRG1 expression, again indicating a stable tissue-Treg phenotype of LTBR-AIR Treg cells (Fig. 5*H* and *SI Appendix*, Fig. S7*C*). Compared with the control Treg cell group, we have seen a tendency toward higher total Nos. of LTBR-AIR Treg cells in the colon (Fig. 5*H*, *Right*). In addition, transferred engineered Treg cells isolated from spleen and colon retained high surface expression of the LTBR-AIR receptor, even at day 47 posttransplantation (Fig. 5*I* and *SI Appendix*, Fig. S7*D*). In summary, these data show that LTBR-AIR Treg

cells are functional and protect mice from GvHD, validating the AIR concept in vivo.

Expression and Functionality of Human LTBR-AIR Treg Cells. To translate the AIR concept into the human setting, a human LTBR-AIR was designed analogous to the mouse version, containing extracellular and transmembrane domains from human LTBR and intracellular signaling domains from human CD28 and CD3-ζ chain (Fig. 6*A*). Naive human Treg cells were isolated from peripheral blood as described before (37) and retrovirally transduced. Human Treg cells efficiently expressed the human LTBR-AIR (hLTBR-AIR) on the cell surface after expansion for 7 d (Fig. 6*B*). Coculture of hLTBR-AIR Treg cells with HEK cells expressing human membrane-bound LIGHT (hLIGHT) induced upregulation of CD137 (4-1BB) and GARP, similar to α-CD3/CD28–stimulated Treg cells (Fig. 6 *C* and *D*). Such an activation was neither detectable in the hLTBR-AIR-negative Treg fraction ($CD90.1^-$) of the same coculture (*SI Appendix*, Fig. S8*A*) nor in Treg cells expressing an irrelevant CAR (α-carcinoembryonic antigen [CEA] CAR) after coculture with HEK-hLIGHT cells (Fig. 6 *C* and *D*). LTBR-AIR Treg cells stimulated with hLIGHT further showed induced expression levels of the activation markers CD69 and CD134 (OX40), as well as of the chemokine receptor CCR8 and LAP (Fig. 6*E*). These results reveal a comparable activation potential of human LTBR-AIR-expressing Treg cells as we demonstrated for murine AIR-Treg counterparts.

These data illustrate that our AIR-Treg concept is translatable to the human system and a viable option for a class of engineered Treg therapies.

Discussion

In this study, we generated artificial receptors that translate an inflammatory ligand signal into a TCR-activating signal. TNF

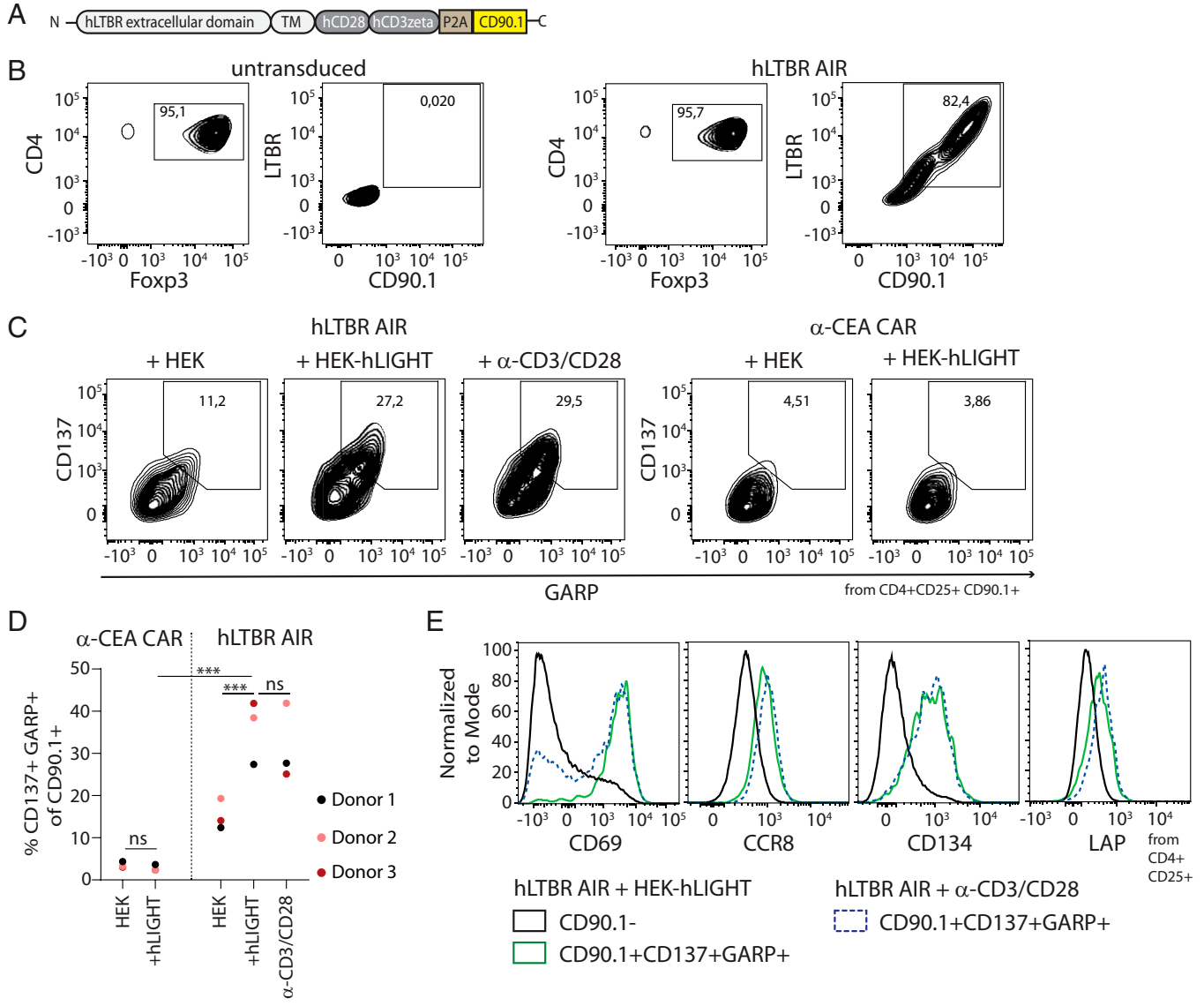

Fig. 6. Human LTBR-AIR expression and signaling capacity. (*A*) Schematic representation of the hLTBR-AIR construct. (*B*) Flow cytometric analysis of transduction efficiency (CD90.1 expression) and hLTBR expression on human $FOXP3^+$ Treg cells 3 d after transduction with hLTBR-AIR construct or on untransduced control Treg cells. (*C*) Flow cytometric analysis of Treg cells expressing hLTBR-AIR or an irrelevant CAR (α-CEA, carcinoembrionic antigen) after 18 h coculture with HEK cells or HEK cells expressing hLIGHT protein on the surface or after stimulation with TransACT (α-CD3/CD28). Representative flow cytometry data from one donor out of three are shown. Gating includes $CD4^+CD25^+CD90.1^{++}$ (about 25% of Treg cells). (*D*) Summary of all three donors. Shown are mean values of two technical replicates per donor (two-way ANOVA) (*E*) Flow cytometric analysis of $CD90.1^-$ and $CD90.1^+$ hLTBR-AIR Treg cells after 18 h of coculture with hLIGHT-expressing HEK cells or after α-CD3/CD28 stimulation. Representative flow cytometry data from one donor out of three are shown. $^*P < 0{,}05$; $^{**}P < 0{,}01$; $^{***}P < 0{,}001$; ns, not sigificant.

superfamily ligands are involved in virtually all autoimmune and chronic inflammatory disease situations. By targeting these ligands, our strategy is to create smart Treg cells that are responsive to inflammation, rather than specific disease-driving antigens, and can therefore be used as a Treg cell–based therapy approach for a broad range of inflammatory diseases.

The interest in engineering Treg cells for therapy is growing rapidly. Biotech and pharmaceutical companies have realized the potential of engineered Treg therapy, and considerable investments are launched in this field (38). For example, Treg cells are engineered specifically against alloantigens to prevent graft rejection after solid-organ transplantation by expression of CARs. Recent reports using xenogeneic/humanized mouse models have thus demonstrated that α-HLA-A2 CAR Treg cells show superior protection in transplant situations when compared with nonengineered polyclonal Treg cell products (11–13). Treg cells equipped with CARs or TCRs are found in organs affected by autoimmunity and inflammation, e.g., the gut (17, 39) or the central nervous system (15); however, focusing on one specific epitope may not be favorable to address autoimmune diseases, which are driven by a large and sometimes even unknown repertoire of autoantigens affecting various organs.

Our AIRs act as environment sensors that trigger TCR-like activation and proliferation of Treg cells in response to TNF ligands independently of their TCR. LTBR-AIR expression and signaling in Treg cells improves protection against GvHD development compared with Treg cells having a polyclonal TCR repertoire only. As LIGHT is mainly expressed by activated B and T cells, especially by transferred donor T cells during GvHD (32), LTBR-AIR Treg activation could occur in both the draining lymphoid organs as well as in the inflamed tissues. That could be an advantage over CAR Treg approaches, where the recognized antigen is mainly expressed at one site, e.g., in a transplant, and not in the draining LNs (11).

Our data also indicate that the choice of the AIR should consider endogenous expression of the receptor, as competition for the ligand or potentially new pairing of AIRs and the endogenous receptor may occur, which might have negative consequences for the Treg activation, as we have seen for the TNFR2-AIR in the RNA-seq data. Therefore, AIRs based on receptors that are not endogenously expressed by the engineered cell type, such as the LTBR-AIR, might be advantageous in this respect.

AIR-mediated conversion of inflammatory signal information provides major advantages over CARs or transduced TCRs: first, the negative effect of proinflammatory cytokines, such as LIGHT and TL1A, can reduce the suppressive capacity of Treg cells (40–44) via endogenous signaling, and this can be reversed into Treg activation by the AIRs. Second, AIR-induced Treg cell activation occurs only at the sites and at the time of inflammation, as AIR signaling cannot be triggered by soluble ligands but only by membrane-bound ligands. Third, a No. of extracellular receptor domains interact with more than one ligand, as, for example, LTBR can bind two ligands $LT\alpha_1\beta_2$ and LIGHT, and this obviously can additionally broaden the functional efficiency. Fourth, advantages of natural receptor domains, such as the ones used here for the AIRs, show a higher stability as compared with CARs that are prone to aggregation via their single-chain variable fragment (scFv). Thereby, CARs can cause a tonic signal in the T cells independently of specific ligand binding (45). Finally, the scFv of the CAR or the interface between scFv and the hinge/transmembrane region may cause immunogenicity, leading to reduced long-term persistence of the CARs (45).

We focused on three members of the TNFR superfamily: LTBR, TNFR2, and DR3. In principle, one could generate additional AIRs targeting a variety of other membrane-bound inflammatory ligands of the TNFR superfamily. Beyond the members of the TNFR superfamily, there are other inflammation-associated receptor families and their respective ligands, which fulfill similar requirements and could be the bases of further AIR constructs, e.g., AIRs recognizing membrane-bound ligands of the epidermal growth factor family or adhesion molecules. Thus, we provide here a synthetic immune receptor concept for engineering Treg cells that are activated by the inflammatory environment, opening therapy options to address various diseases with (multiorgan) inflammation.

Materials and Methods

Ethics Statement. Peripheral blood mononuclear cells for T cell enrichment were isolated from leukocyte reduction chambers from healthy donors donating thrombocytes. Collection of immune cells from donors was performed in compliance with the Helsinki Declaration after ethical approval by the local ethical committee (Regensburg University, reference No. 19-1614-101) and signed informed consent.

Mice. Female BALB/c mice, C57BL/6 Nr4a1-eGFP mice (JAX stock No. 016617, C57BL/6-Tg(Nr4a1-EGFP/cre)820Khog/J) and C57BL/6 CD45.1$^+$ mice (JAX stock No. 002014, B6.SJL-Ptprc^{a}Pepc^b/BoyCrl) were obtained from Charles River Breeding Laboratories (Wilmington, MA, USA) or the Jackson Laboratory (Bar Harbor, ME, USA). B6N.129(Cg)-Foxp3^{tm3Ayr} mice (Foxp3.IRES-DTR/GFP) were bred to C57BL/6 CD45.1$^+$ mice and served as BM donors for GvHD experiments. C57BL/6 Foxp3-hCD2 (Foxp3$^{tm1(CD2/CD52)Shori}$) was a gift from S. Hori (46).

Design of AIRs. Murine and human AIRs were designed according to published nucleotide sequences (https://www.ensembl.org/). Extracellular and transmembrane domains of LTBR, DR3, and TNFR2 were fused to the intracellular signaling domains of CD28 and the CD3-ζ chain. Two point mutations were introduced into the murine CD3-ζ chain, as they were shown to increase expression of CARs (47). As negative control, an open reading frame (ORF) was used, coding for transmembrane and signaling domain of CD28 and the signaling domain of the CD3-ζ chain. The α-CD19 CAR as well as the α-CEA CAR have been described previously (48, 49). The HLA-A2 CAR construct is based on published sequence (GenBank: MP143507.1). ORFs coding for the AIRs as well as the α-CD19 CAR, the α-HLA A2 CAR, and the α-CEA CAR were fused to the congenic marker CD90.1 by ligating to a self-cleaving P2A sequence. cDNAs were synthesized by ThermoFisher/Life Technologies and cloned into the pMSCV-Thy1.1 retroviral backbone (Addgene, cat No. 17442) via NotI/MluI. Nucleotide sequences are depicted in *SI Appendix*.

Digestion of Murine Tissues for Flow Cytometric Analysis, Fluorescence-Activated Cell Sorting (FACS) of Cells and Transplantation. To isolate cells from colon tissue, colons were isolated, cleared of feces, and prepared according to manufacturer's instructions with the lamina propria dissociation kit (Miltenyi Biotec) and gentleMACS device (Miltenyi Biotec, program 37C_mLPDK_1). More-detailed protocols about T cell isolation from murine tissues are published (50) and described in *SI Appendix*.

Flow Cytometry and FACS. Flow cytometry samples were acquired on a BD FACSymphony, a BD FACSCelesta, or a BD LSRII flow cytometer. Cell sorting was performed with a BD FACSAriaII or BD FACSFusion cell sorter with 70-μm nozzle (details in *SI Appendix*).

Culture and Retroviral Transduction of Treg Cells. Retroviruses in the pMSCV-Thy1.1 system were manufactured in Phoenix-Eco cells, a pCLEco (packaging plasmid)-carrying variant of HEK293 cells (details in *SI Appendix*).

Treg Proliferation Assay. α-CD3/CD28 beads were removed from transduced Treg cultures via MACSiMAG separator magnet. Treg cells were rested for 18 h in fresh medium supplemented with 100 U/mL rhIL-2. Treg cells were labeled with CellTrace CFSE Cell Proliferation dye (1 μM) and added onto HEK293 cells expressing mTNF, mTL1A, or mLIGHT. rhIL-2 (2,000 U/mL) was added to the cell cultures. After 72 h of coincubation, proliferation of transduced CFSE-labeled Treg cells was analyzed via flow cytometry.

RNA-Seq and Bioinformatics. Total RNA was isolated using the Qiagen RNeasy Micro Kit, and RNA was eluted in 14 μL RNase-free water. RNA quality was assessed

using the Tapestation system 4200 and High-Sensitivity RNA screentape (Agilent). Seven microliters of the RNA was used for generating RNA-seq libraries using the SMART-seq Stranded Kit from Takara. Indexed libraries were pooled in an equimolar ratio and sequenced on an Illumina NextSeq 550 machine with NextSeq 500/550 High Output Kit v2.5 (75 cycles). Quality control and read mapping to the mouse reference genome (GRCm38, gencode, release23) was performed using an adapted version of the SnakePipes analysis pipeline (v1.2.2 including rDNA removal). Mapping was performed using STAR, and gene counts are based on featureCounts.

Quality control of the count matrix and differential expression gene calling was performed with *DESeq2*. Gene counts were imported and prefiltered with *edgeR:filterByExpr*, and the false discovery rate (FDR) was set to 0.05. gene ontology analysis was performed with genes upregulated with a log2 fold change > 1 and FDR < 0.05 using *goseq*. Gene set enrichment analysis was performed using *fgsea*. Plots were created with *ggplot2* and *EnhancedVolcano* (51).

GvHD Model. BALB/c (H-2K^d) recipients were irradiated (8 Gy) and transplanted retrobulbar with 2.5×10^6 BM cells with or without (BM control) 5×10^5 splenocytes from C57BL/6 CD45.1$^+$ donors (H-2K^b). The animals in the therapy groups received 2.5×10^5 in vitro expanded and transduced C57BL/6 Treg (Foxp3-hCD2 reporter, CD45.2$^+$). Recipients were monitored daily and body weight and GvHD symptoms assessed two or three times weekly by non-blinded investigators applying standardized scoring protocols (approved by Committee on Ethics of Animal Experiments at the Bavarian Government, details in *SI Appendix*).

Statistical Analysis. Data were analyzed with Prism software or algorithm. Statistical details are indicated in the figure legend. For survival differences, Kaplan–Meier analysis was performed and the log-rank test was used. Statistics for RNA-seq is as described in *SI Appendix, Materials and Methods*. $P < 0.05$ was considered significant ($^*P < 0.05$; $^{**}P < 0.01$; $^{***}P < 0.001$).

Data, Materials, and Software Availability. Correspondence and requests for materials should be addressed to Markus Feuerer.

The main data supporting the results in this study are available within the paper and its supplementary material. The accession No. for the RNA-seq data reported in this paper is Gene Expression Omnibus GSE197477.

[RNA-seq data] data have been deposited in [Gene Expression Omnibus] (GSE197477) (52).

ACKNOWLEDGMENTS. Sequencing and bioinformatic analysis were conducted at the NGS Core Unit of the Leibniz Institute for Immunotherapy (LIT). We thank the flow cytometry core facility of the LIT and the animal facility of the University of Regensburg for technical support. We thank H. Stanewsky, J. Raithel, U. Ackermann, D. Weber-Steffens, M. Wuttke, R. Eder, and I. Fink for technical support. We thank S. Hori for Foxp3-hCD2 mice. This work was supported by grants from the European Research Council (ERC-CoG, No. 648145 REGiREG) to M.F. This work was funded by the Deutsche Forschungsgemeinschaft (German Research Foundation) Projektnummer 324392634-TRR 221 to M.F.

Author affiliations: [a]Leibniz Institute for Immunotherapy, 93053 Regensburg, Germany; [b]Chair for Immunology, Universität Regensburg, 93053 Regensburg, Germany; [c]Institute of Immunology, Universitätsmedizin Mainz, 55131 Mainz, Germany; and [d]Department of Internal Medicine III, Universitätsklinikum Regensburg, 93053 Regensburg, Germany

1. S. Sakaguchi *et al.*, Regulatory T cells and human disease. *Annu. Rev. Immunol.* **38**, 541–566 (2020).
2. M. Panduro, C. Benoist, D. Mathis, Tissue Tregs. *Annu. Rev. Immunol.* **34**, 609–633 (2016).
3. C. Campbell, A. Rudensky, Roles of regulatory T cells in tissue pathophysiology and metabolism. *Cell Metab.* **31**, 18–25 (2020).
4. M. Delacher *et al.*, Single-cell chromatin accessibility landscape identifies tissue repair program in human regulatory T cells. *Immunity* **54**, 702–720.e17 (2021).
5. M. Delacher *et al.*, Precursors for nonlymphoid-tissue Treg cells reside in secondary lymphoid organs and are programmed by the transcription factor BATF. *Immunity* **52**, 295–312.e11 (2020).
6. M. Romano, G. Fanelli, C. J. Albany, G. Giganti, G. Lombardi, Past, present, and future of regulatory T cell therapy in transplantation and autoimmunity. *Front. Immunol.* **10**, 43 (2019).
7. J. A. Bluestone, Q. Tang, T_{reg} cells-the next frontier of cell therapy. *Science* **362**, 154–155 (2018).
8. B. R. Blazar, K. P. A. MacDonald, G. R. Hill, Immune regulatory cell infusion for graft-versus-host disease prevention and therapy. *Blood* **131**, 2651–2660 (2018).
9. L. M. R. Ferreira, Y. D. Muller, J. A. Bluestone, Q. Tang, Next-generation regulatory T cell therapy. *Nat. Rev. Drug Discov.* **18**, 749–769 (2019).
10. N. A. J. Dawson *et al.*, Functional effects of chimeric antigen receptor co-receptor signaling domains in human regulatory T cells. *Sci. Transl. Med.* **12**, 1–16 (2020).
11. A. Sicard *et al.*, Donor-specific chimeric antigen receptor Tregs limit rejection in naive but not sensitized allograft recipients. *Am. J. Transplant.* **20**, 1562–1573 (2020).
12. K. G. MacDonald *et al.*, Alloantigen-specific regulatory T cells generated with a chimeric antigen receptor. *J. Clin. Invest.* **126**, 1413–1424 (2016).
13. F. Noyan *et al.*, Prevention of allograft rejection by use of regulatory T cells with an MHC-specific chimeric antigen receptor. *Am. J. Transplant.* **17**, 917–930 (2017).
14. D. A. Boardman *et al.*, Expression of a chimeric antigen receptor specific for donor HLA class I enhances the potency of human regulatory T cells in preventing human skin transplant rejection. *Am. J. Transplant.* **17**, 931–943 (2017).
15. M. Fransson *et al.*, CAR/FoxP3-engineered T regulatory cells target the CNS and suppress EAE upon intranasal delivery. *J. Neuroinflammation* **9**, 112 (2012).
16. D. Wu *et al.*, A method for expansion and retroviral transduction of mouse regulatory T cells. *J. Immunol. Methods* **488**, 112931 (2021).
17. D. Blat, E. Zigmond, Z. Alteber, T. Waks, Z. Eshhar, Suppression of murine colitis and its associated cancer by carcinoembryonic antigen-specific regulatory T cells. *Mol. Ther.* **22**, 1018–1028 (2014).
18. J. Skuljec *et al.*, Chimeric antigen receptor-redirected regulatory T cells suppress experimental allergic airway inflammation, a model of asthma. *Front. Immunol.* **8**, 1125 (2017).
19. M. Croft *et al.*, TNF superfamily in inflammatory disease: Translating basic insights. *Trends Immunol.* **33**, 144–152 (2012).
20. J. L. Browning, Inhibition of the lymphotoxin pathway as a therapy for autoimmune disease. *Immunol. Rev.* **223**, 202–220 (2008).
21. Y. Yu, P. Jiang, P. Sun, N. Su, F. Lin, Analysis of therapeutic potential of preclinical models based on DR3/TL1A pathway modulation (Review). *Exp. Ther. Med.* **22**, 693 (2021).
22. S. Bittner, M. Ehrenschwender, Multifaceted death receptor 3 signaling-promoting survival and triggering death. *FEBS Lett.* **591**, 2543–2555 (2017).
23. A. B. Kunnumakkara *et al.*, Upside and downside of tumor necrosis factor blockers for treatment of immune/inflammatory diseases. *Crit. Rev. Immunol.* **39**, 439–479 (2019).
24. A. Borelli, M. Irla, Lymphotoxin: From the physiology to the regeneration of the thymic function. *Cell Death Differ.* **28**, 2305–2314 (2021).
25. B. A. Osborne *et al.*, Identification of genes induced during apoptosis in T lymphocytes. *Immunol. Rev.* **142**, 301–320 (1994).
26. E. H. Lee *et al.*, Axl acts as a tumor suppressor by regulating LIGHT expression in T lymphoma. *Oncotarget* **8**, 20645–20655 (2017).
27. R. Lin *et al.*, USP4 interacts and positively regulates IRF8 function via K48-linked deubiquitination in regulatory T cells. *FEBS Lett.* **591**, 1677–1686 (2017).
28. W. Lee, H. S. Kim, S. Y. Baek, G. R. Lee, Transcription factor IRF8 controls Th1-like regulatory T-cell function. *Cell. Mol. Immunol.* **13**, 785–794 (2016).
29. J. M. Moreau, M. Velegraki, C. Bolyard, M. D. Rosenblum, Z. Li, Transforming growth factor-β1 in regulatory T cell biology. *Sci. Immunol.* **7**, eabi4613 (2022).
30. M. Edinger *et al.*, CD4+CD25+ regulatory T cells preserve graft-versus-tumor activity while inhibiting graft-versus-host disease after bone marrow transplantation. *Nat. Med.* **9**, 1144–1150 (2003).
31. C. Riegel *et al.*, Efficient treatment of murine acute GvHD by in vitro expanded donor regulatory T cells. *Leukemia* **34**, 895–908 (2020).
32. Y. Xu *et al.*, Selective targeting of the LIGHT-HVEM costimulatory system for the treatment of graft-versus-host disease. *Blood* **109**, 4097–4104 (2007).
33. K. Tamada *et al.*, Modulation of T-cell-mediated immunity in tumor and graft-versus-host disease models through the LIGHT co-stimulatory pathway. *Nat. Med.* **6**, 283–289 (2000).
34. C. Zhang *et al.*, Dynamic changes in serum cytokine levels and their clinical significance in predicting acute GVHD. *Oncotarget* **8**, 53691–53700 (2017).
35. Y. Shono *et al.*, Bone marrow graft-versus-host disease: Early destruction of hematopoietic niche after MHC-mismatched hematopoietic stem cell transplantation. *Blood* **115**, 5401–5411 (2010).
36. M. Delacher *et al.*, Genome-wide DNA-methylation landscape defines specialization of regulatory T cells in tissues. *Nat. Immunol.* **18**, 1160–1172 (2017).
37. P. Hoffmann *et al.*, Only the CD45RA+ subpopulation of CD4+CD25high T cells gives rise to homogeneous regulatory T-cell lines upon in vitro expansion. *Blood* **108**, 4260–4267 (2006).
38. E. Dolgin, T_{reg} engineers take aim at autoimmunity. *Nat. Biotechnol.* **39**, 1317–1319 (2021).
39. E. Elinav, N. Adam, T. Waks, Z. Eshhar, Amelioration of colitis by genetically engineered murine regulatory T cells redirected by antigen-specific chimeric receptor. *Gastroenterology* **136**, 1721–1731 (2009).
40. H. Nie *et al.*, Phosphorylation of FOXP3 controls regulatory T cell function and is inhibited by TNF-α in rheumatoid arthritis. *Nat. Med.* **19**, 322–328 (2013).
41. A. Zanin-Zhorov *et al.*, Protein kinase C-theta mediates negative feedback on regulatory T cell function. *Science* **328**, 372–376 (2010).
42. X. Valencia *et al.*, TNF downmodulates the function of human CD4+CD25hi T-regulatory cells. *Blood* **108**, 253–261 (2006).
43. S. Q. Khan *et al.*, Cloning, expression, and functional characterization of TL1A-Ig. *J. Immunol.* **190**, 1540–1550 (2013).
44. Y. Wang, M. Zhu, P. Yu, Y. X. Fu, Promoting immune responses by LIGHT in the face of abundant regulatory T cell inhibition. *J. Immunol.* **184**, 1589–1595 (2010).
45. G. M. Branella, H. T. Spencer, Natural receptor- and ligand-based chimeric antigen receptors: Strategies using natural ligands and receptors for targeted cell killing. *Cells* **11**, 1–25 (2021).
46. N. Komatsu *et al.*, Heterogeneity of natural Foxp3+ T cells: A committed regulatory T-cell lineage and an uncommitted minor population retaining plasticity. *Proc. Natl. Acad. Sci. U.S.A.* **106**, 1903–1908 (2009).
47. P. Nguyen, I. Moisini, T. L. Geiger, Identification of a murine CD28 dileucine motif that suppresses single-chain chimeric T-cell receptor expression and function. *Blood* **102**, 4320–4325 (2003).
48. A. A. Hombach, G. Rappl, H. Abken, Blocking CD30 on T cells by a dual specific CAR for CD30 and colon cancer antigens improves the CAR T cell response against CD30$^-$ tumors. *Mol. Ther.* **27**, 1825–1835 (2019).
49. J. N. Kochenderfer, Z. Yu, D. Frasheri, N. P. Restifo, S. A. Rosenberg, Adoptive transfer of syngeneic T cells transduced with a chimeric antigen receptor that recognizes murine CD19 can eradicate lymphoma and normal B cells. *Blood* **116**, 3875–3886 (2010).
50. A. Cossarizza *et al.*, Guidelines for the use of flow cytometry and cell sorting in immunological studies (second edition). *Eur. J. Immunol.* **49**, 1457–1973 (2019).
51. V. Bhardwaj *et al.*, snakePipes: Facilitating flexible, scalable and integrative epigenomic analysis. *Bioinformatics* **35**, 4757–4759 (2019).
52. S. Bittner, M. Feuerer, N. Strieder, Artificial Immune Receptors as novel tools to engineer inflammation sensing regulatory T cells for cell therapy. NCBI: GEO. https://www.ncbi.nlm.nih.gov/geo/query/acc.cgi?acc=GSE197477. Deposited 25 February 2022.